J Eng Math (2008) 62:277–287
DOI 10.1007/s10665-007-9211-1

The similarity regime for natural convection in a vertical cylindrical well filled with an anisotropic porous medium

G. Degan · M. Gibigaye · C. Akowanou · N. C. Awanou

Received: 6 October 2006 / Accepted: 19 December 2007 / Published online: 15 January 2008

Abstract An integral method based on Lighthill's analysis (Q J Mech Appl Math 6 (1953) 398–439) is carried out to study the similarity regime for penetration of convective heat transfer in a vertical cylindrical well filled with an anisotropic porous medium. The porous medium is anisotropic in permeability with its principal axes oriented in a direction that is oblique to the gravity vector. In the limit of the slenderness of the porous matrix, the penetration length of the convective flow and the heat-transfer rate are expressed in terms of the anisotropic properties of the porous medium, the modified Darcy–Rayleigh number and the aspect ratio of the geometrical configuration. A scale analysis is applied to predict the order of magnitudes involved in the similarity regime of the phenomenon. The conditions of existence of the similarity pattern is found to be dependent on the anisotropic parameters. It is demonstrated that both the anisotropic permeability ratio and the orientation angle of the principal axes have a strong influence on the heat-transfer rate and on the vertical penetration length into the well.

Keywords Anisotropic porous medium · Convection · Darcy–Rayleigh number · Penetrative flows

1 Introduction

Natural convection in fluid-saturated porous media is of considerable importance in engineering. Applications include convection in the Earth's crust, flows in soils, aquifers, petroleum extraction, storage of agriculture products, insulation techniques, and geothermal energy extraction. The state of the art has been reviewed by Cheng [1].

A few studies have been made on convective heat transfer about a vertical cylinder embedded in a porous medium. Minkowycz and Cheng [2] have done an analysis on natural convective flow about a vertical cylinder embedded in a saturated porous medium, where the surface temperature of the cylinder varies as a power function of distance from the leading edge. Exact and approximate solutions based on local similarity and local non-similarity models were obtained within the framework of boundary-layer approximations. Vasantha and Nath [3] have studied numerically, by a finite-difference scheme and using also the method of extended perturbation series, the thermal boundary

G. Degan (✉) · M. Gibigaye · C. Akowanou
Ecole Polytechnique d'Abomey-Calavi, LEMA, B.P. 2009, Cotonou, Bénin
e-mail: ger_degan@yahoo.fr

N. C. Awanou
Faculté des Sciences et Techniques, LPR, B.P. 526, Cotonou, Bénin

layer along an isothermal cylinder in a porous medium. They have found that the thermal boundary-layer thickness increases as the transverse curvature parameter of the cylinder increases. Bejan ([4], [5, pp. 403–407]) has studied analytically natural convection in a vertical cylindrical well filled with a porous medium, when the impermeable surface may have concavities filled by the neighboring porous material. That author was the first to demonstrate that an important feature of the similarity flow is that the depth to which the free-convection pattern penetrates the well is proportional to the temperature difference driving the flow.

All previous studies have usually been concerned with homogeneous isotropic porous structures. The inclusion of more physical realism in the matrix properties of the medium is important for the accurate modeling of anisotropic media. Anisotropy, which is generally a consequence of a preferential orientation or asymmetric geometry of the grain of fibers, is in fact encountered in numerous systems in industry and nature. Natural soils of river beds are considered as geological systems with anisotropic sediments and rocks. Following Bear [6, Sect. 5.2], sediments are commonly deposited such that their permeability in the horizontal directions (unless tilting of the formation occurs) is greater than in other directions. River beds can be idealized as an anisotropic porous medium underlying the fluid layer exposed to atmosphere and whose upper free boundary is permeable and thermally heated by solar radiation. According to Neale [7], many porous media are encountered in practice, especially those formed as a result of industrial geological sedimentation processes are anisotropic in constitution, for example, filter beds, river beds, drilling mud cakes, underground rock formations, and soil sands. That is to say, their measured macroscopic transport properties, such as permeability, diffusivity, and electrical conductivity, are direction-dependent. Anisotropy is generally a consequence of the preferential orientation and asymmetric geometry of the grains which constitute the porous medium. Despite this, natural convection in such anisotropic porous media has received relatively little attention. The critical Rayleigh number for the onset of convection was first considered by Castinel and Combarnous [8] who conducted an experimental and theoretical investigation for a layer with impermeable boundaries. The effect of thermal anisotropy on the onset of motion was studied by Epherre [9]. Kvernvold and Tyvand [10] extended these analyses to supercritical finite-amplitude convection. McKibbin [11] conducted an extensive study on the effects of anisotropy on the convective stability of a porous layer. At the upper surface of the porous medium, he considered boundary conditions sufficiently general to allow both impermeable and constant-pressure boundaries. Tyvand and Storesletten [12] investigated the problem concerning the onset of convection in an anisotropic porous layer in which the principal axes were obliquely oriented to the gravity vector. As a result, new flow patterns with a titled plane of motion or titled lateral cell walls were obtained. Convective heat transfer in a vertical anisotropic porous cavity heated from the side with various thermal boundary conditions have been investigated by Zhang [13], Degan et al. [14] and Degan and Vasseur [15,16]. It was demonstrated that the heat transfer was maximum when the principal axis with higher permeability is parallel to the vertical direction, and minimum when it is perpendicular. Recently, Nield and Kuznetsov [17–20] have investigated the effects of combined vertical and horizontal heterogeneity on the onset of convection in a bidisperse porous medium and the results obtained for the physical problem are of significant importance to many geophysical and engineering-related applications.

The objective of the present paper is to outline an analysis of the anisotropic influence on the natural-convection phenomenon in a vertical cylindrical well filled with an anisotropic porous medium. The porous medium is anisotropic in permeability with its principal axes oriented in a direction that is oblique to the gravity vector. Also, anisotropy in thermal conductivity is considered with its principal axes coincident with the coordinate directions. For the similarity regime, the governing equations in the limit of the slenderness of the cavity are solved analytically.

2 Mathematical formulation

The physical model considered here in Fig. 1 consists of a two-dimensional vertical cylindrical well of elongated shape filled with a porous medium composed of a sparse distribution of particles completely surrounded by a saturating fluid. The well opens into a semi-infinite reservoir filled with the same porous medium. As considered in nature in fact, the porous medium is anisotropic in flow permeability. The permeabilities along the two principal axes of the porous matrix are denoted by K_1 and K_2. The anisotropy in flow permeability of the porous medium is

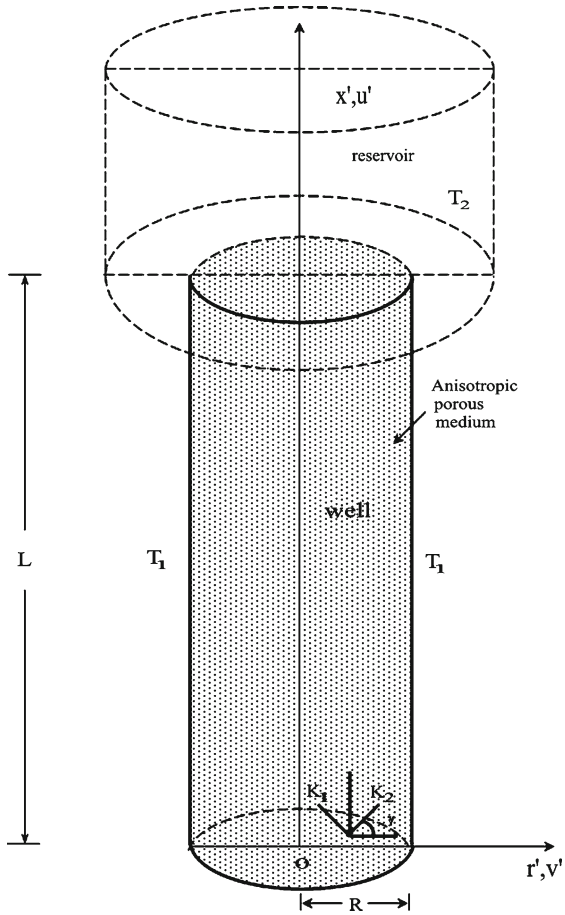

Fig. 1 Schematic of a cylindrical porous well and coordinate system

characterized by the permeability ratio $K^* = K_1/K_2$ and the orientation angle γ, defined as the angle between the horizontal direction and the principal axis with permeability K_2. The rotation takes place about the horizontal line (i.e., the r-axis) from which the anisotropic rotation angle γ is encountered. Consequently, the cylindrical polar coordinates (r, x) identified as the Cartesian coordinate system (r, x) are used in the present analysis as the framework and then the flowfield will be axisymmetric. The porous vertical cylinder is bounded by two rigid vertical side walls heated at the constant temperature T_1, while the semi-infinite reservoir situated above the well is relatively colder ($T_2 < T_1$). This is a potentially unstable configuration which leads to fluid motion, cold fluid falling into the well through the middle of the circular cross-section and warmer fluid rising along the heated cylindrical wall. The saturating fluid is viscous, incompressible and assumed to be in local thermodynamic equilibrium with the porous medium everywhere. The thermophysical properties of the fluid are assumed constant, except for the density in the buoyancy term in the momentum equation (Boussinesq approximation).

Under the above approximations, the equations describing the laminar and two-dimensional steady convective flow in an anisotropic porous medium can be written as follows (see Bear [6])

$$\nabla.\vec{V}' = 0, \tag{1}$$

$$\vec{V}' = \frac{\overline{\overline{K}}}{\mu}(-\nabla p' + \varrho\vec{g}), \tag{2}$$

$$(\varrho c_p)_f \nabla.(\vec{V}'T') = k\nabla^2 T', \tag{3}$$

where $\vec{V}'$ in the superficial flow velocity, T' the temperature, p' the pressure, $\vec{g}$ the gravitational acceleration, $(\varrho c)_f$ the heat capacity of the saturating fluid, μ the dynamic viscosity, ϱ the density and k the thermal conductivity. The symmetrical second-order permeability tensor $\overline{\overline{K}}$ is defined as

$$\overline{\overline{K}} = \begin{bmatrix} K_1 \cos^2\gamma + K_2 \sin^2\gamma & (K_1 - K_2)\sin\gamma\cos\gamma \\ (K_1 - K_2)\sin\gamma\cos\gamma & K_2\cos^2\gamma + K_1\sin^2\gamma \end{bmatrix}. \tag{4}$$

In physical variables, the previous governing equations 1–3 and the equation of state (expressed by the Boussinesq approximation) can be rewritten as follows

$$\frac{\partial}{\partial r'}(r'v') + \frac{\partial}{\partial x'}(r'u') = 0, \tag{5}$$

$$au' - cv' = -\frac{K_1}{\mu}\left(\frac{\partial p'}{\partial x'} + \varrho g\right), \tag{6}$$

$$-cu' + bv' = -\frac{K_1}{\mu}\left(\frac{\partial p'}{\partial r'}\right), \tag{7}$$

$$u'\frac{\partial T'}{\partial x'} + v'\frac{\partial T'}{\partial r'} = \alpha\left\{\frac{1}{r'}\frac{\partial}{\partial r'}\left(r'\frac{\partial T'}{\partial r'}\right) + \frac{\partial^2 T'}{\partial x'^2}\right\}, \tag{8}$$

$$\varrho = \varrho_1[1 - \beta(T' - T_1)], \tag{9}$$

where

$$a = \cos^2\gamma + K^*\sin^2\gamma, \quad b = \sin^2\gamma + K^*\cos^2\gamma, \quad c = \frac{1}{2}(1 - K^*)\sin 2\gamma \tag{10}$$

and u' and v' are the velocity components in the x'- and r'-directions; $\alpha = k/(\varrho c_p)_f$ is the thermal diffusivity of the fluid.

Eliminating the pressure term by taking the curl of (6) and (7) and making use of (5), we obtain a single momentum equation, which reads as follows:

$$a\frac{\partial u'}{\partial r'} + c\left(\frac{\partial u'}{\partial x'} - \frac{\partial v'}{\partial r'}\right) - b\frac{\partial v'}{\partial x'} = \frac{K_1 g\beta}{\nu}\frac{\partial T'}{\partial r'}. \tag{11}$$

The appropriate boundary conditions prevailing at the solid cylindrical wall are

$$\begin{aligned} &r' = R: \quad v' = 0, \quad T' = T_1, \quad (a) \\ &x' = 0: \quad u' = 0, \quad T' = T_1, \quad (b) \end{aligned} \tag{12}$$

where R is the well radius.

It is convenient after a brief scale analysis to renormalize the governing equations by introducing the following transformations:

$$x = x'/L, \quad r = r'/R, \quad u = u'R^2/(\alpha L), \quad v = v'R/\alpha, \quad T = \frac{K_1 g\beta L(T' - T_1)}{\alpha\nu}\left(\frac{R}{L}\right)^2. \tag{13}$$

Substituting the above variables in (5), (8) and (11), we find that the dimensionless governing equations of conservation of mass, momentum and energy in steady-state are

$$\frac{\partial u}{\partial x} + \frac{v}{r} + \frac{\partial v}{\partial r} = 0, \tag{14}$$

$$a\frac{\partial u}{\partial r} + c\left(\frac{R}{L}\right)\left(\frac{\partial u}{\partial x} - \frac{\partial v}{\partial r}\right) - b\left(\frac{R}{L}\right)^2\frac{\partial v}{\partial x} = \frac{\partial T}{\partial r}, \tag{15}$$

$$u\frac{\partial T}{\partial x}+v\frac{\partial T}{\partial r}=\left(\frac{\partial^2 T}{\partial r^2}+\frac{1}{r}\frac{\partial T}{\partial r}\right)+\left(\frac{R}{L}\right)^2\frac{\partial^2 T}{\partial x^2}. \tag{16}$$

In dimensionless terms, the boundary conditions (12a) and (12b) at the wall become

$$\begin{aligned} &r=1: \quad v=0, \quad T=0, \quad (a),\\ &x=0: \quad u=0, \quad T=0, \quad (b). \end{aligned} \tag{17}$$

Because of the slenderness of the well, $(R/L)\ll 1$, (L being the well height) and therefore, in the dimensionless governing equations (14–16), the terms multiplied by the well aspect ratio (R/L) can be considered negligible. Consequently, using the scales of the variables of interest presented in (13), it is clear that the present analysis is valid if the conditions

$$\frac{a}{c}\gg\frac{R}{L} \tag{18}$$

and

$$\frac{a}{b}\gg\left(\frac{R}{L}\right)^2 \tag{19}$$

are satisfied.

Considering the boundary condition at the line where the well communicates with the semi-infinite and large porous reservoir, we assume that the centerline temperature at the mouth of the well equals the reservoir (see Bejan [4]),

$$x=1: \quad r=0, \quad T=-\mathrm{Ra}_L\left(\frac{R}{L}\right)^2, \tag{20}$$

where Ra_L the Darcy–Rayleigh number based on the height L of the well, is defined by

$$\mathrm{Ra}_L=\frac{K_1 g\beta L(T_1-T_2)}{\alpha\nu}. \tag{21}$$

3 Solution

Following Lighthill [21] and Bejan [4], we observe that a similarity solution is posssible upon examining the governing equations (14–16), for which a natural convection pattern exists when the velocity and temperature radial profiles have the same shape independent of vertical position. But, both the velocity and temperature longitudinal distributions u and T are proportional to x while v is a function of radial position only. So, the similarity regime observed is similar to that found by Lighthill [21] while studying natural convection in vertical tubes filled with fluid and revisited by Bejan [5, pp. 403–407] for the same problem in a well filled with an isotropic porous medium. Due to the nonlinearity associated with the convection terms in the energy equation (16), exact analytical solutions for u, v and T are impossible. So, following the previous analyses reported here, one can seek solutions satisfying the condition (20) without the $(R/L)^2$ term in an integral fashion and at specified locations, along the centerline $r=0$ and the wall $r=1$:

$$\frac{\mathrm{d}}{\mathrm{d}x}\left(\int_0^1 ruT\,\mathrm{d}r\right)=\left(\frac{\partial T}{\partial r}\right)\Big|_{r=1}, \tag{22}$$

$$\left(u\frac{\partial T}{\partial x}\right)\Big|_{r=0}=\left(\frac{\partial^2 T}{\partial r^2}+\frac{1}{r}\frac{\partial T}{\partial r}\right)\Big|_{r=0}, \tag{23}$$

$$0=\left(\frac{\partial^2 T}{\partial r^2}+\frac{1}{r}\frac{\partial T}{\partial r}\right)\Big|_{r=1}. \tag{24}$$

Moreover, from the continuity equation (14), the following condition has to be satisfied:

$$\int_0^1 ur \, \mathrm{d}r = 0 \tag{25}$$

The next step is the selection of reasonable profiles for the velocity and temperature distributions that satisfy the momentum equation (15) identically. Generally, polynomial expressions for temperature and vertical velocity are more suitable. So, making use of the following expressions

$$T = x(m_0 + m_2 r^2 + m_4 r^4 + m_6 r^6), \tag{26}$$

$$u = \frac{x}{a}(n_0 + m_2 r^2 + m_4 r^4 + m_6 r^6), \tag{27}$$

we observe that (15) is identically satisfied and obtain five equations for five unknown coefficients appearing in the expressions (26) and (27). These unknown coefficients are determined from the conditions (17a) and (22–25). The results depending upon the anisotropic parameters are obtained after lengthy algebraic manipulations and are expressed as follows:

$$\begin{cases} m_2 = \dfrac{24 m_0^2}{7m_0 + 240a}, & m_4 = -\dfrac{3m_0(17m_0 + 144a)}{7m_0 + 240a}, \\ m_6 = \dfrac{4m_0(5m_0 + 48a)}{7m_0 + 240a}, & n_0 = \dfrac{96 a m_0}{7m_0 + 240a}, \end{cases} \tag{28}$$

where $m_0 = -11.81038a$. It is obvious that in the limit of an isotropic porous medium for which $a = 1$, the result of (28) is in agreement with that obtained by Bejan [4].

The continuity equation is automatically satisfied by introducing the stream function ψ as

$$ru = \frac{\partial \psi}{\partial r}, \quad rv = -\frac{\partial \psi}{\partial x}. \tag{29}$$

As pointed out by Bejan [4], an important feature of the similarity flow is that the depth to which the free-convection pattern penetrates the well is proportional to the temperature difference driving the flow. It is convenient to predict an order of magnitude for this vertical penetration distance of convection into the well. To determine the scale of the vertical penetration length L_x, one can obtain from governing equations (5), (8) and (11) the following balances

$$\frac{u'}{L_x} \sim \frac{v'}{R}, \tag{30}$$

$$a\frac{u'}{R} \sim \frac{K_1 g\beta}{\nu}\frac{\Delta T}{R}, \tag{31}$$

$$v'\frac{\Delta T}{R} \sim \alpha \frac{\Delta T}{R^2}. \tag{32}$$

Because of the slenderness of the well, we assume that the vertical penetration occurs over a distance L_x that is greater than R. Combining (30–32), we write the scales of the quantities of interest as follows:

$$u' \sim \alpha L^{-1} a^{-1} \mathrm{Ra}_L, \tag{33}$$

$$v' \sim \alpha^{-1} R, \tag{34}$$

$$L_x \sim L a^{-1} \mathrm{Ra}_L \left(\frac{R}{L}\right)^2. \tag{35}$$

To express completely the physical length of the similarity pattern denoted here by ℓ_s, one can make use of the thermal condition (20) combined with the temperature distribution (26) to have

$$\frac{\ell_s}{L} = -\frac{1}{m_0}\mathrm{Ra}_L \left(\frac{R}{L}\right)^2, \tag{36}$$

which becomes

$$\frac{\ell_s}{L} = 0.08467 \frac{\mathrm{Ra}_L}{a} \left(\frac{R}{L}\right)^2. \tag{37}$$

It is clear from (37) that the physical length of the penetration of the convective flow into the well depends upon the anisotropic parameters of the porous matrix. So, as long as $\ell_s \preceq L$, a similarity pattern will exist in the well [4] if the following condition

$$\mathrm{Ra}_L \left(\frac{R}{L}\right)^2 \preceq 11.81a \tag{38}$$

holds.

The net heat-transfer interaction between the wall of the vertical cylindrical well and the semi-infinite reservoir is defined by the Nusselt number Nu which can be expressed in physical variables as follows:

$$\mathrm{Nu} = \frac{Q}{kL(T_1 - T_2)}, \tag{39}$$

where the heat flux upward through the mouth of the well is

$$Q = \int_0^R (\varrho c_p)_f u'T' \mathrm{d}(\pi r'^2) = 2\pi (\varrho c_p)_f \left(\int_0^R r'u'T' \mathrm{d}r'\right)_{x'=L}, \tag{40}$$

which represents the heat flux transferred through the mouth of the well situated at $x' = L$. Taking into account Eqs. (30) and (31), we have that the scale of the heat-transfer rate Nu is given by

$$\mathrm{Nu} \sim a^{-1} \mathrm{Ra}_L \left(\frac{R}{L}\right)^2 \tag{41}$$

Using equations (13) and (36), we can rewrite the heat-transfer rate in dimensionless terms as

$$\mathrm{Nu} = \frac{2\pi}{\mathrm{Ra}_L \left(\frac{R}{L}\right)^2} \left(\int_0^1 ruT \mathrm{d}r\right)_{x=1}. \tag{42}$$

Substitution of (26), (27) and (37) in (42) yields the heat-transfer rate in the similarity regime:

$$\mathrm{Nu} = \frac{0.255}{a} \mathrm{Ra}_L \left(\frac{R}{L}\right)^2. \tag{43}$$

It is obvious that the results obtained for the penetration length of convection, Eq. (37), and for the Nusselt number, Eq. (43), are in agreement with those found by the scale-analysis prediction through (31) and (41), respectively.

4 Results and discussion

First, in order to test the validity of this study, a model of the flow pattern inside the vertical cylindrical well is presented, as shown before [4]. Therefore, Fig. 2 illustrates the streamline (ψ = constant) pattern in the similarity regime of the convective heat flow in the region of vertical penetration into the porous cavity, for $K^* = 1.0$ and $\gamma = 0°$ (case corresponding to an isotropic porous medium for which $a = 1$). Indeed, combining Eqs. (27) and (29), one can obtain that the streamline pattern in the similarity regime is calculated by $\psi = (xr/a) * [n_0 + m_2(r^2/3) + m_4(r^4/5) + m_6(r^6/7)]$ = constant for given values of r and of x such that, when $K^* = 1.0$ (i.e., $a = 1$); the result obtained for this particular situation corresponding to the isotropic porous medium is in agreement with that found by Bejan [4]. Thus, choosing the same values of the streamlines presented by this author, Fig. 2 drawn for the values of $\psi/(-0.7215)$, indicates that the observed flow fields are the same as those obtained by Bejan [4]. As the vertical impermeable wall of the well is relatively cold ($T = 0$), comparing it to the centerline temperature, which is assumed to be concident with that of the reservoir above and at the mouth of the well, cold fluid creeps down the

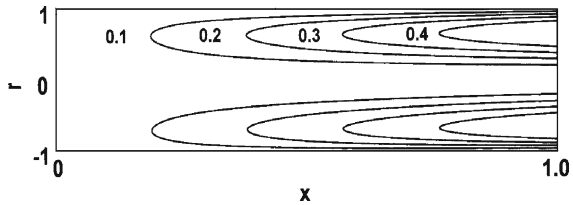

Fig. 2 Streamline pattern ($\psi/(-0.7215) = \text{constant}$) in the similarity regime

centerline, gradually warming up the further it reaches into the well. At the same time a layer of warmer fluid rises along the cylindrical wall, resulting in channeling the flow and hydrodynamic boundary-layer thickness along that wall.

Now, the effects of anisotropic permeability on the temperature field will be analyzed. Figure 3a–c illustrate the effects of the permeability ratio K^* on the isotherms [$T/(-0.7215) = \text{constant}$] presented for $\gamma = 45°$. For $K^* = 1.0$, Fig. 3a shows the temperature fields in the isotropic porous situation. In general, as a result, counter-clockwise rotating cells penetrate into the cylindrical cavity at $x = 1.0$, by a side of the cross-section from the centerline and move out by the opposite half cross-section side at the mouth of the well. A symmetry of the cells with respect to the centerline ($r = 0$) and thermal boundary layers along the vertical isothermal wall is then observed. As the well is slender enough, apart from the penetration region inside the vertical cylinder, a stagnant fluid zone ahead of the penetration zone is observed. The temperature variation is seen to be large in the vertical boundary thermal regions along the cylindrical wall when the value of the isotherm is made weaker and, consequently, the isotherm whose value is weaker penetrates more and more into the well. Upon decreasing K^* from 1 to 0.25, it is seen from Fig. 3b that all the isotherms move out progressively from their penetration zone when compared with the isotropic situation. For example, the isotherm [$T/(-0.7215) = 1$] moves out from $x \approx 0.12$–0.18 on the centerline of the well, while the isotherm [$T/(-0.7215) = 3$] moves out from $x \approx 0.37$–0.93 and are found to be more concentrated in the core region, in the neighbourhood of the warmer centerline. This behavior can be explained by the fact that, for fixed values of γ and [$\text{Ra}_L(R/L)^2$] (i.e., K_1), a decrease in K^* can be interpreted as an increase in the permeability K_2, resulting in an enhancement of the temperature field. Naturally, the reverse is true when K^* is made greater than unity. Thus, Fig. 3c shows that for $K^* = 2.5$, all the isotherms are strongly channeled along the vertical boundary wall which is relatively cold, indicating that the resulting heat transfer is weak. It follows from these results that a large permeability ratio ($K^* > 1$) causes a weakness of the convective heat transfer inside the cylinder, while a small permeability ratio ($K^* < 1$) causes the strength of the temperature field. This is a logical consequence of the vertical penetration of the phenomenon to which attention has to be paid later on.

In Fig. 4, the average heat transfer, Nu, is given as a function of [$\text{Ra}_L/(R/L)^2$] for selected values of the anisotropic orientation γ and for $K^* = 10$. The curves obtained here for different values of γ are seen as straight and parallel lines, because of the logarithmic scale adopted for the coordinate axes. They are all valid only for the similarity regime, according to the condition of existence of the similarity pattern predicted by Eq. (38) which depends on the anisotropic parameter, a ($= \cos^2\gamma + K^* \sin^2\gamma$). Because of this condition, all the curves presented in Fig. 4 break off at a value of Nu which is independent of the anisotropic properties of the porous matrix. Indeed, making use of Eq. (43) and the condition (38), one can demonstrate that $\text{Nu} \preceq 3.0115$; this is the limiting value of the convective heat-transfer rate penetrating the cylindrical well over which the similarity regime will cease to exist. For each curve corresponding to a given value of the anisotropic orientation γ, one can derive the condition of the existence of the similarity regime of the convective heat transfer. For example, for $\gamma = 15°$, this condition is formulated by [$\text{Ra}_L(R/L)^2 \preceq 18.93$], while for $\gamma = 45°$, [$\text{Ra}_L(R/L)^2 \preceq 65.95$]. These limits are drawn as dotted lines in the figure.

Figure 5 shows the influence of the anisotropic permeability ratio K^* on the penetration length (ℓ_s/L) of the convective heat transfer into the cylindrical well for $\gamma = 45°$. It is seen that, for a given value of K^*, the penetration length increases progressively, as the parameter [$\text{Ra}_L/(R/L)^2$] depending on the heating process increases, to reach a value which depends upon the anisotropic properties of the porous medium. As expected, in the Eq. (37), (ℓ_s/L)

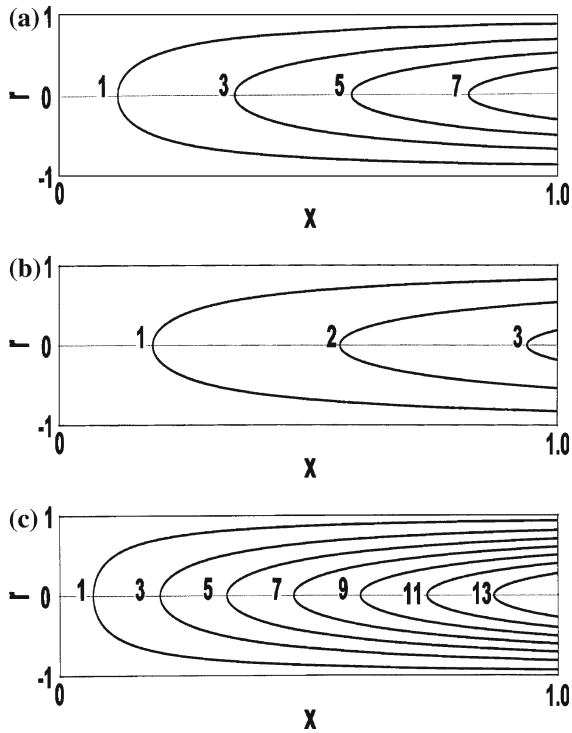

Fig. 3 Isotherm pattern ($T/(-0.7215) = \text{constant}$) in the similarity regime for (**a**) $K^* = 1$ and for $\gamma = 45°$, (**b**) $K^* = 0.25$ and for $\gamma = 45°$, (**c**) $K^* = 2.5$ and for $\gamma = 45°$

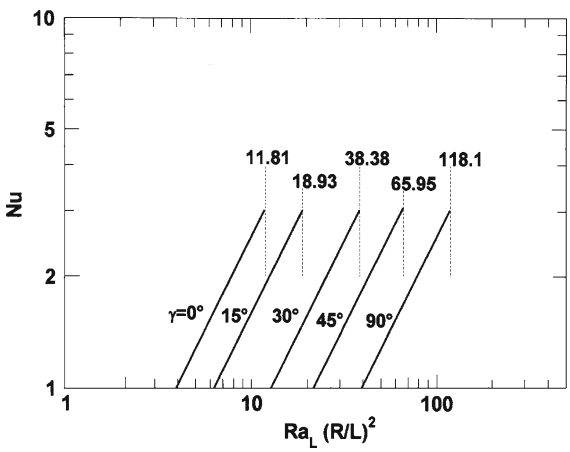

Fig. 4 Effect of the orientation angle of principal axes γ and the parameter $\mathrm{Ra}_L(R/L)^2$ on the heat-transfer rate, in the similarity regime

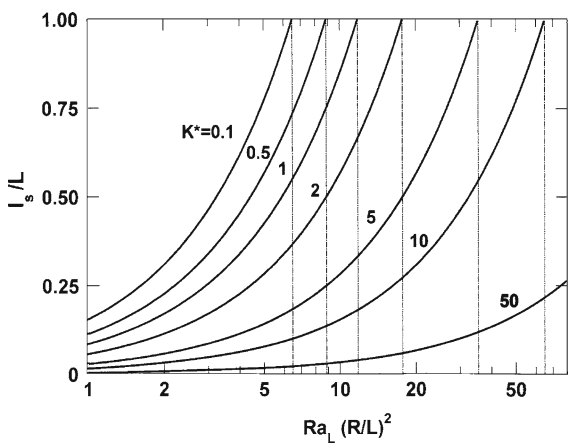

Fig. 5 Effect of the anisotropic permeability ratio K^* and the parameter $\mathrm{Ra}_L(R/L)^2$ on the vertical penetration of convection into the well, in the similarity regime

does depend on the parameter a, a function of K^* and γ. Moreover, the limiting value of $[\mathrm{Ra}_L/(R/L)^2]$ presented as a dotted line for each selected value of K^*, providing the condition of existence of the similarity regime is predited by Eq. (38). It is observed that, for a fixed value of $[\mathrm{Ra}_L/(R/L)^2]$, the penetration length of the buoyancy-induced flow decreases more and more when $K^* > 1$ and increases more and more for the situations where $K^* < 1$. This behavior can be explained by the fact that, for a given value of $[\mathrm{Ra}_L/(R/L)^2]$, (i.e., of K_1), an increase in K^* can be interpreted by an increase of the parameter a, and as the latter is inversely proportional to the penetration length

(see Eq. (37)), therefore (ℓ_s/L) has to be decreasing. Naturally, the reverse trend is achieved when $K^* < 1$. For $K^* = 1$, we have $a = 1$ and the result is found to be in excellent agreement with that obtained by Bejan [4].

5 Conclusions

A study has been made of the penetration phenomenon of natural convective heat transfer in a vertical cylindrical well filled with a porous medium. The porous medium is assumed to be hydrodynamically anisotropic with the principal axes of anisotropic permeability inclined with respect to the gravity force. An analytical solution, valid for flow in slender enclosures, is derived on the basis of an integral method used by Lighthill [21] in his analysis of natural convection in vertical tubes filled with fluid. Detailed results for the flow field, temperature distribution, penetration length of convection into the well and heat-transfer rate have been presented and analyzed. From these results, the following remarks can be made:

1. Both the permeability ratio and inclination angle of the principal axes have a strong influence on the vertical penetration of thermal convection in the anisotropic porous cylindrical well.
2. A large permeability ratio ($K^* > 1$) causes a weakness of the convective heat transfer inside the cylinder and a large penetration length of convection, while a small permeability ratio ($K^* < 1$) determines the strength of the temperature field and the weakness of the penetration length of the convective flow.

The interaction of finite-size, heated, porous layers with a localized source of heat constitutes a class of buoyancy-induced flows through anisotropic porous media which is encountered in practice in groundwater hydrology, oil reservoirs, soil science, chemical engineering and many other branches of engineering and science. The penetrative-flow problems considered in confined porous layers with one side permeable, communicating with a fluid reservoir heated differentially are new research subjects which have to be tackled on the basis of different orientations of the physical configurations in order to investigate influences of the physical properties of the porous solid matrix on the buoyancy-induced flow.

Appendix: Nomenclature

a, b, c	Constants, Eq. (10)
c_p	Specific heat of fluid at constant pressure
$\vec{g}$	Gravitational acceleration
k	Thermal conductivity
$\overline{\overline{K}}$	Flow permeability tensor, Eq. (4)
K_1, K_2	Flow permeability along the principal axes
K^*	Anisotropic permeability ratio, K_1/K_2
L	Height of the well
L_x	Vertical penetration length
ℓ_s	Physical length of the similarity pattern
Nu	Nusselt number, Eq. (43)
p	Pressure
Q	Heat flux, Eq. (40)
R	Radius of the well
Ra_L	Darcy–Rayleigh number, Eq. (21)
T	Temperature
$\vec{V}$	Seepage velocity
u, v	Velocity components in x, r-directions
x, r	Cylindrical coordinates

Greek symbols

α	Thermal diffusivity
β	Thermal expansion coefficient of the fluid
ΔT	Characteristic scale of temperature
μ	Dynamic viscosity of the fluid
ψ	Stream function
γ	Inclination angle of principal axes
ϱ	Density of the fluid
(ϱc_p)	Heat capacity of the fluid

Superscript

$'$	Physical variables

References

1. Cheng P (1978) Heat transfer in geothermal systems. Adv Heat Transfer 15:1–105
2. Minkowycz WJ, Cheng P (1976) Free convection about a vertical cylinder embedded in a porous medium. Int J Heat Mass Transfer 19:805–813
3. Vasantha R, Nath G (1987) Forced convection along a longitudinal cylinder embedded in a saturated porous medium. Int Comm Heat Mass Transfer 14:639–646
4. Bejan A (1980) Natural convection in a vertical cylindrical well filled with porous medium. Int J Heat Mass Transfer 23:726–729
5. Bejan A (1984) Convection heat transfer. Wiley-Interscience Publication
6. Bear J (1972) Dynamics of fluids in porous media. Dover Publications, New York
7. Neale G (1977) Degrees of anisotropy for fluid flow and diffusion (electrical conduction) through anisotropic porous media. AIChE J 23:56–62
8. Castinel G, Combarnous M (1974) Critère d'apparition de la convection naturelle dans une couche poreuse anisotrope. C R Hebd Seanc Acad Sci Paris B 278:701–704
9. Epherre J F (1975) Critère d'apparition de la convection naturelle dans une couche poreuse anisotrope. Rev Gen Therm 168: 949–950
10. Kvernvold O, Tyvand PA (1979) Nonlinear thermal convection in anisotropic porous media. J Fluid Mech 90:609–624
11. McKibbin R (1984) Thermal convection in a porous layer: effects of anisotropy and surface boundary conditions. Trans Porous Media 1:271–292
12. Tyvand P, Storesletten L (1991) Onset of convection in an anisotropic porous medium with oblique principal axes. Heat transfer Jpn Res 22:139–153
13. Zhang X (1993) Convective heat transfer in a vertical porous layer with anisotropic permeability. In: Proc 14th Canadian congr appl mech Vol 2, pp 579–580
14. Degan G, Vasseur P, Bilgen E (1995) Convective heat transfer in a vertical anisotropic porous layer. Int J Heat Mass Transfer 38:1975–1987
15. Degan G, Vasseur P (1996) Natural convection in a vertical slot filled with an anisotropic porous medium with oblique principal axes. Numer Heat Transfer A 30:397–412
16. Degan G, Vasseur P (1997) Boundary-layer regime in a vertical porous layer with anisotropic permeability and boundary effects. Int J Heat Fluid Flow 18:334–343
17. Nield DA, Kuznetsov AV (2007) The effect of combined vertical and horizontal heterogeneity on the onset of convection in a bidisperse porous medium. Int J Heat Mass Transfer 50:3329–3339
18. Nield DA, Kuznetsov AV (2007) The onset of convection in a shallow box occupied by a heterogeneous porous medium with constant flux boundaries. Trans Porous Media 67:441–451
19. Nield DA, Kuznetsov AV (2007) The effects of combined horizontal and vertical heterogeneity on the onset of convection in a porous medium. Int J Heat Mass Transfer 50:1909–1915
20. Nield DA, Kuznetsov AV (2006) The onset of convection in a bidisperse porous medium. Int J Heat Mass Transfer 49:3068–3074
21. Lighthill MJ (1953) Theoretical considerations on free convection in tubes. Q J Mech Appl Math 6:398–439